Korean J. Chem. Eng., 40(12), 3087-3095 (2023)
DOI: 10.1007/s11814-023-1576-y

pISSN: 0256-1115
eISSN: 1975-7220

Vanadium redox flow batteries including carbon catalysts derived from low-density polyethylene and polyurethane

Hyeonsoo Lim*,‡, Mingyu Shin,‡, and Yongchai Kwon*,**,†**

*Department of New and Renewable Energy Convergence, Seoul National University of Science and Technology, 232, Gongneung-ro, Nowon-gu, Seoul 01811, Korea
**Department of Chemical and Biomolecular Engineering, Seoul National University of Science and Technology, Nowon-gu, Seoul, 01811, Korea
(*Received 2 August 2023 • Revised 8 September 2023 • Accepted 22 September 2023*)

Abstract−Utilizing waste plastic to produce carbon catalysts is one way to recycle waste plastic. Carbon catalysts derived from low-density polyethylene (LDPE) (LDPE-C catalyst) and polyurethane (PUK-C catalyst) can help to improve the performance of vanadium redox flow batteries (VRFBs). Especially, for forming the PUK-C catalyst that has abundant surface nitrogen functional groups and large surface area, carbonization process is needed. Electrochemical analysis discloses that when this PUK-C catalyst is doped onto graphite felt (GF), the reactivity for redox reactions of vanadium ions is significantly enhanced. Specifically, peak current density and peak potential separation for the redox reactions are more improved than those observed with bare GF. Additionally, charge transfer resistance for the redox reactions is reduced when using PUK-C catalyst doped GF. When the performance of VRFBs utilizing PUK-C catalyst doped GF is measured, they exhibit better energy efficiency than VRFBs operated without the catalyst by 8.1%. Furthermore, maximum power density of VRFBs utilizing PUK-C catalyst doped GF can generate 14.9% higher power at 30 mA cm^{-2} than that of VRFBs utilizing bare felt. These findings demonstrate that the PUK-C catalyst is highly effective in enhancing the performance of VRFBs.

Keywords: Vanadium Redox Flow Battery, Low-density Polyethylene, Polyurethane, Carbon, Catalyst

INTRODUCTION

Various efforts have been made to reduce carbon emissions due to serious environmental pollution issue. As a result, demands for generating the electrical energy or electricity using renewable energies instead of conventional fossil fuels are growing because the fossil fuels can induce high carbon emissions [1]. However, since renewable energies are intermittent and not uniform, large-scale energy storage devices are necessary to provide the electricity produced from the renewable energies to consumers steadily [2].

Among the large-scale energy storage devices, redox flow batteries (RFBs) have advantages in durability because their electrodes are not directly involved in desirable redox reactions, and electrolyte can be reused for a long time by its rebalancing. Furthermore, these RFBs can adjust the capacity and power sector independently by controlling the size of tanks and electrodes. In particular, they are far safer from fires and explosions than other conventional energy storage devices because they use aqueous electrolytes [3-8].

Of the RFBs, the most popular one has been vanadium RFBs (VRFBs) to date. VRFBs utilize vanadium ions as active materials for both catholyte and anolyte. Due to use of the same active materials for both electrolytes, they can be rebalanced irrespective of crossover, which is very beneficial point because the rebalancing of active materials can make them reusable for a longer time. More specifically, the charging and discharging in cathode of VRFB occur due to the redox reactions of VO^{2+}/VO_2^+ ions, while those in anode occur due to the redox reactions of V^{2+}/V^{3+} ions [9-18]. However, despite their outstanding benefits, VRFBs are not commercially established due to their current limitation and relatively low performance.

Numerous studies have been conducted to enhance the performance of VRFBs by addressing the limitations. Significant efforts have been made to develop electrodes and catalysts that can improve the reactivity for redox reactions of vanadium ions, which is key factors affecting the performance of VRFBs [9-18]. Metal and metal oxide catalysts, including Bi, Nb, and Mn, have been predominantly considered so far. However, although the metal catalysts could provide excellent durability and performance under strong acidic electrolytes, they were usually expensive and toxic due to by-products produced for their charging and discharging [19,20].

As an alternative, carbon-based catalysts have been suggested and investigated. Carbon-based catalysts require high conductivity and exceptionally excellent stability. Carbon nanotubes, graphene, and activated carbon have been commonly employed for this purpose [8,11,16,17]. Sun et al. employed dopamine as a nitrogen source for doping multi-walled carbon nanotubes with carboxylic functional groups (CACNTs), which was subsequently applied to VRFBs. The incorporation of this catalyst into graphite felt (GF) resulted in better energy efficiency (EE) and capacity utilization than unmodified GF [21]. Similarly, Chung et al. modified the surface of CACNT using

†To whom correspondence should be addressed.
E-mail: kwony@seoultech.ac.kr
‡H. Lim and M. Shin contributed equally to this work.

urea and citric acid as precursors. By the precursor ratios, an optimal composition was determined and the optimal one was applied to VRFBs [11]. In a related study, Kothandaraman et al. used activated carbon extracted from sugarcane bagasse for use as anodic catalyst in VRFBs. Notably, the catalyst exhibited large surface area and a diverse array of hydrophilic functional groups, making it a promising candidate for VRFBs. Moreover, the biomass-derived catalyst could be prepared with low cost [22].

Among various carbon-based catalysts, activated carbons offer better cost benefits than other carbon materials, while they can be easily fabricated using cheap raw materials or by introducing desirable functional groups through heat and acidic treatments [23-25]. Notably, utilizing waste plastics to produce the activated carbons can be favorable in an environmental aspect because the use of waste plastics can provide a proper solution for treating with plastic wastes that are a main cause of environmental pollutions. Even in a prospect of cost, utilizing the waste plastics for production of the expensive activated carbons can save the cost.

Plastics can be classified into thermoplastic and thermosetting types. In previous study, we produced carbon catalyst using LDPE that is thermoplastic plastic [26-28]. LDPE is famous for its softness and flexibility, which are attributed to its low density. Due to the property, LDPE can be simply processed. Thus, this has already been used for diverse industries including vinyl, coatings, and cables, and has been produced in substantial quantities. Consequently, the significant amount of waste LDPE has been generated as by-product occurring for the fabrication process of its extensive products. In contrast to this, the process of thermosetting plastics is not simple, while its recycling options are very limited. Among the thermosetting plastics, there is polyurethane. This has a three-dimensional structure and has been used for insulator, thermal barrier, and sound absorber [29-34]. Regarding its component, the polyurethane has nitrogen functional groups, and the groups act as active sites promoting desirable redox reactions of vanadium ions in VRFBs [10,15,35,36]. In particular, graphitic nitrogen functional groups exhibited a notably high negative charge density owing to a strong electronegativity of such incorporated nitrogen atoms. This property promoted the adsorption of positively charged vanadium ions and further provided active sites for activating redox reactions of vanadium ions. Additionally, the extra electrons imported by the nitrogen dopant formed localized electronic states near to the dopant site. These states acted as the vacant molecular orbitals of VO^{2+} or VO_2^+, facilitating the formation of nitrogen-vanadium transitional state. The transitional states then promoted electron transfer between vanadium ions and catalyst, optimizing the redox reactions of vanadium ions [37].

Based on these considerations, this study proposes a method to recycle both waste LDPE and polyurethane by utilizing them as catalysts promoting the desirable redox reactions of vanadium ions in VRFBs. To achieve this goal, they undergo a carbonization process, converting them into valuable carbon catalysts. However, LDPE consists of long polymer chains, resulting in weak thermal stability. Consequently, relying solely on heat treatment makes it difficult to complete the carbonization process. Therefore, it is crucial to enhance the initial thermal stability of LDPE. In the previous study, we used chemical methods to achieve this [27]. According to the chemical methods, a crosslinking step that enabled the mutual connection of polymer chains within LDPE using sulfuric acid was newly introduced. The crosslinking of polymer chains enhanced their bond strength, improving the thermal stability of LDPE.

With that, the subsequent carbonization step was ready to be carried out. During heating, polyurethane underwent thermal degradation, and thus, byproducts such as methanol and acetic acid were produced by the thermally degraded polyurethane. Since the polyurethane was a thermosetting plastic, this became difficult to process it in thermally degraded state. In this study, to address this issue, potassium carbonate was further included, and the mixture of polyurethane and potassium carbonate was heated. Here, the potassium carbonate was acted as cross-linking agent, and this facilitated the formation of cross-linking structure between polymer chains, enhancing their thermal stability and preventing the undesirable side reactions. Furthermore, the potassium carbonate can further react with carbon atoms of its surface, and the reaction facilitated surface etching, increasing its surface area [38-43].

In summary, this study focuses on modifying plastics to produce carbon catalysts for improvement in the performance of VRFBs. These carbon catalysts have better advantages than similar materials due to their large active surface area, excellent surface porosity, and increase in a portion of desirable functional groups that help to increase the reactivity for redox reactions of vanadium ions. To assess the effects of these carbon catalysts on the performance of VRFBs, various characterizations and VRFB single cell tests were conducted.

EXPERIMENTAL

1. Materials

A low density polyethylene (LDPE, Sigma Aldrich, 0.925 g/mL at 25 °C) and polyurethane (Goodfellow, Nominal granule size of 3-5 mm) were used as precursors. Sulfuric acid (SAMCHUN, 95%) was used for electrolyte and crosslinking of LDPE. Potassium carbonate (Sigma Aldrich, 99%) was used for carbonization of polyurethane. Vanadium (IV) oxide sulfate hydrate (Sigma Aldrich, 97%) was used as active material. Isopropyl alcohol (IPA, SAMCHUN, 99.0%) was used for dispersion and doping of catalysts.

2. Production of Carbon Catalyst from Plastics

In the production of carbon catalysts using LDPE that is denoted as LDPE-C catalyst, a mixture of 3 g LDPE and 4.5 mL of 95% sulfuric acid was heated at 170 °C for 1 h. The resulting solution then suffered from a cleaning process using deionized water (DIW) (Stabilization step). Following the cleaning step, carbonization was proceeded. The sample for carbonization was initially heated at 900 °C with a ramping rate of 10 °C/min for 1 h under H_2 (5%) and Ar (95%) mixed gas (Carbonization step).

To produce carbon catalysts using polyurethane that is denoted as PUK-C catalyst, 3 g polyurethane was mixed with 3 g potassium carbonate in 3 mL DIW for 24 h. The mixture was subsequently dried at 60 °C under vacuum condition for 24 h. After drying, carbonization was carried out at 800 °C with a ramping rate of 10 °C/min for 1 h under H_2 (5%) and Ar (95%) mixed gas (Carbonization step). Once the sample was cooled to room temperature, this was washed with DIW to eliminate any residual potassium carbon-

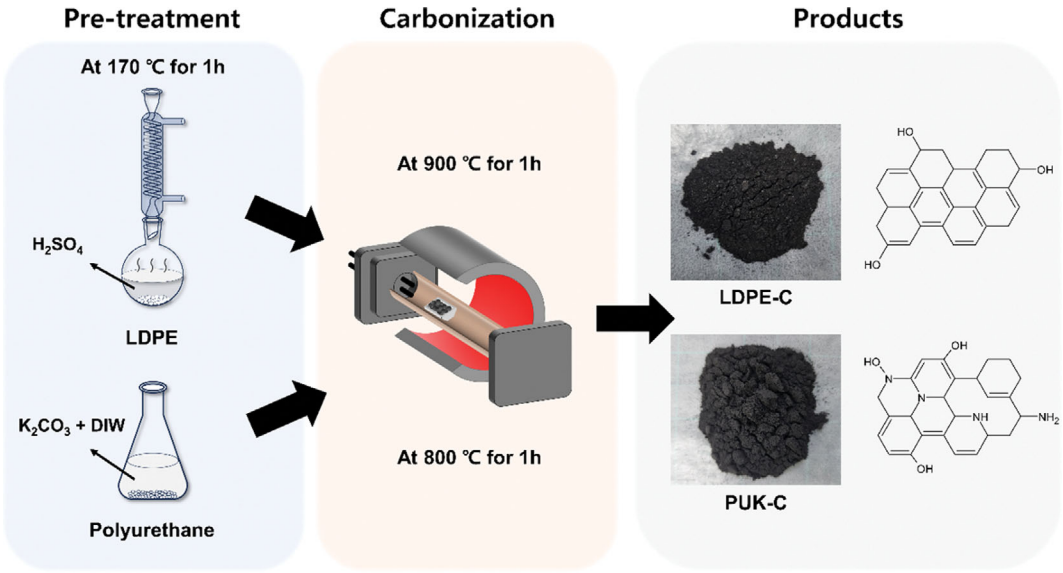

Scheme 1. Illustrations showing the entire process for the production of carbon catalysts.

ate, and then dried in a vacuum oven.

3. Chemical Characterizations of Carbon Catalysts

Raman spectra were measured using a Laser Raman Spectrophotometer (NRS-5100) to verify the successful carbonization of LDPE and polyurethane. The surface area of LDPE-C and PUK-C samples was determined using a Physisorption-Micropore, Mesopore Analyzer (3flex, Micromeritics, USA). To recognize a proper doping of the carbon catalysts onto GF electrode, Scanning Electron Microscope (SEM, JSM-7610F, JEOL) was used. X-ray Photoelectron Spectroscopy (XPS, K-Alpha+, Thermo Scientific) was utilized to analyze the composition of the carbon catalysts. In particular, N1s spectrum of PUK-C exhibited four prominent peaks corresponding to pyridinic, pyrrolic, graphitic and oxidized nitrogen at 398.5, 400.1, 401.1, and 402.4 eV, respectively [29,35,44-46].

4. Electrochemical Characterizations of Activated Carbons

Cyclic voltammetry (CV) and electrochemical impedance spectroscopy (EIS) were carried out using a Bio-Logic VSP-128 potentiostat. A three-electrode cell configuration was employed with GF electrodes of 1 cm diameter acting as working electrode. Pt wire and a silver chloride electrode (Ag/AgCl) were used as counter and reference electrodes, respectively.

CV curves were measured to observe peak current density and peak potential separation of the corresponding samples. The voltage scan rate for the CV measurements was 10 mV/s. The voltage scan range for cathode was 0.4 to 1.35 V (vs. Ag/AgCl), while that of anode was −0.8 to −0.2 V (vs. Ag/AgCl). Regarding the preparation of electrolytes, catholyte was prepared by dissolving 0.015 M $VOSO_4$ into 3 M sulfuric acid, while anolyte was prepared by the electrochemical reduction of catholyte that was in V^{3+} ion state. For EIS measurements, Nyquist plots were measured for anode at 0.9 V and cathode at −0.6 V (vs. Ag/AgCl). The frequency range for the tests was 10 mHz to 200 kHz.

VRFB single cell tests and polarization curves that measured maximum power density (MPD) were conducted using bare and catalyst doped electrodes. The electrode area utilized for the tests was 2×2 cm^2, employing GF and Nafion 117 (Chemours, USA) as electrode material and membrane, respectively. During the activation step of electrolytes, a mixture of 1.5 M vanadium sulfate and 3 M sulfuric acid solution was prepared. Catholyte and anolyte tanks were filled with 17 mL and 15 mL of the mixed solution, respectively. The charging step was initiated with a cut-off voltage of 1.7 V. After completing the activation step, catholyte was removed, and the catholyte tank was refilled with 15 mL of fresh vanadium solution containing vanadium sulfate and sulfuric acid [47]. In the step tests of VRFB single cells, five cycles were performed at 80, 120, 160, and 200 mA cm^{-2}, respectively.

RESULTS AND DISCUSSION

1. Production of Carbon Catalysts Using Plastics

Although melting point of LDPE is approximately 120 °C, to achieve successful carbonization of LDPE, LDPE should be heat treated at 800 °C or higher temperature. Here, to avoid the undesirable melting or vaporizing of LDPE without being carbonized, its preliminary modification is also needed. With the preliminary modification, improving the thermal stability of LDPE is also important. To enhance the thermal stability, chemical crosslinking was considered. Regarding the chemical crosslinking, there have been several previous reports. In these reports, LDPE was heat treated at 170 °C for 1 h with sulfuric acid, and as a result, the crosslinking of LDPE chains was successfully completed. Heat treatment of LDPE that was performed at 170 °C under sulfuric acid enabled heat penetration throughout the polymer chains of LDPE, as a result, well-crosslinked and stabilized LDPE structure were formed. Following the stabilization step, carbonization of LDPE was carried out with heat treatment performed at 900 °C for 1 h under H_2 (5%) and Ar (95%) mixed gas.

In contrast to LDPE, the main elements of polyurethane are carbon, nitrogen, oxygen, and hydrogen, which may induce liquid-type by-products like acetic acid and methanol during its carbon-

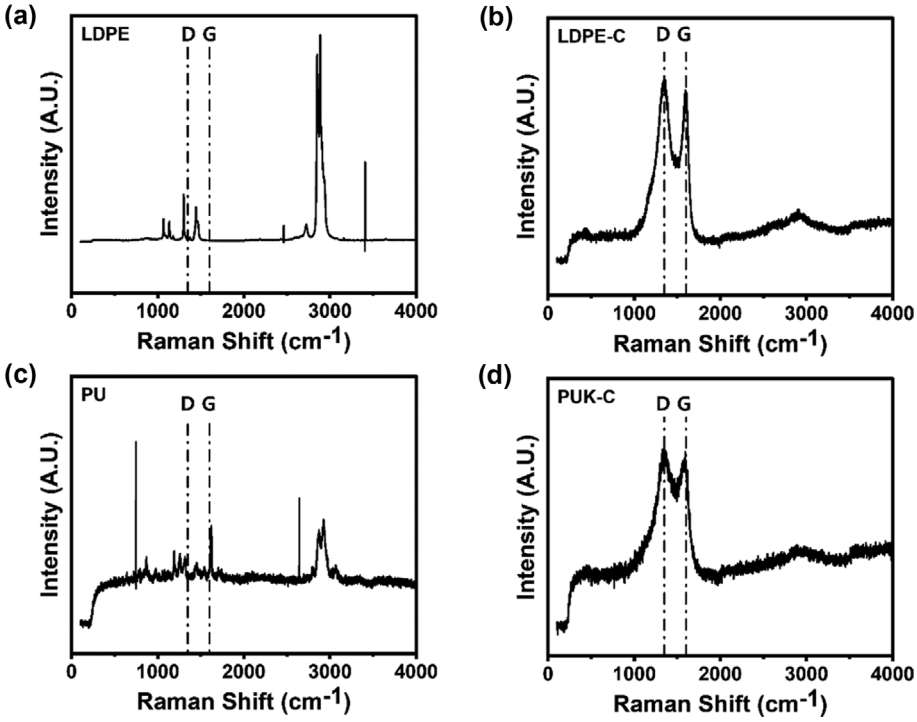

Fig. 1. Raman spectra of (a) LDPE, (b) LDPE-C, (c) PUK, and (d) PUK-C samples.

ization. To suppress the production of by-products, potassium carbonate is further included to polyurethane because it is known that the crosslinking of polyurethane links is promoted when potassium carbonate is involved. Additionally, the reaction between potassium carbonate and carbon can lead to the formation of pores, increasing active surface area [39-42]. Here, the carbonized LDPE and polyurethane samples are denoted as LDPE-C and PUK-C samples.

2. Physical and Chemical Property Evaluation of Carbon Powder

Raman spectra were considered to assess the carbon structure of LDPE, LDPE-C, polyurethane, and PUK-C samples (Fig. 1). As shown in Fig. 1, the characteristic D and G band peaks, which are indicators of typical carbon structure, were not observed in LDPE and polyurethane samples. However, these peaks were clearly observed in LDPE-C and PUK-C samples. This pattern was well matched with the previous researches. According to the previous reports, D and G band peaks of Raman spectra are observed when the carbonized structure is well formed. Based on that, this Raman data is an evidence that both LDPE and polyurethane are successfully carbonized as LDPE-C and PUK-C [28-30].

Regarding the carbonization of LDPE and polyurethane, it is meaningful to measure their surface area of LDPE-C and PUK-C samples because the surface area approximately determines the number of active site of the corresponding sample and the reactivity of desirable redox reactions of active materials. The surface area of the two samples was measured by using the nitrogen adsorption-desorption method based on the Brunauer-Emmett-Teller (BET) theory, and the result is presented in Fig. 2. The analysis revealed that LDPE-C and PUK-C samples exhibited a surface area of 256.4 $m^2 g^{-1}$ and 297.5 $m^2 g^{-1}$ respectively, meaning that their specific surface area was

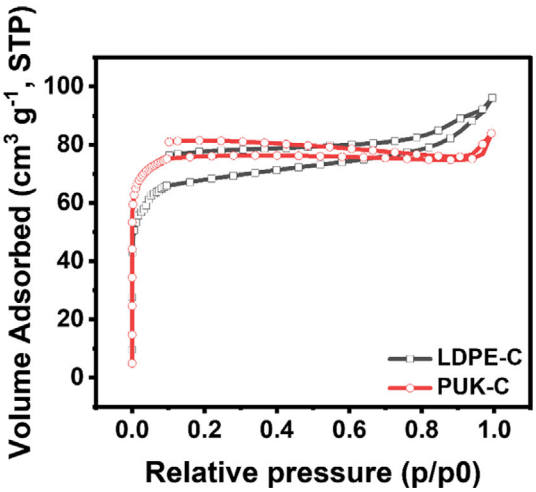

Fig. 2. BET adsorption-desorption isotherm graphs of LDPE-C and PUK-C samples.

similar.

Besides BET analysis, XPS analysis is performed to identify the presence of nitrogen functional groups doped onto surface of the catalysts during carbonization (Fig. 3). As shown in Fig. 3 and Table 1, XPS analysis disclosed that a proportion of nitrogen functional groups included in LDPE-C sample was close to zero, while that of PUK-C sample was 1.8%. As already expected, this is an evidence that polyurethane includes some amount of nitrogen functional groups on its surface after carbonization.

The above analyses provided valuable insights, demonstrating that LDPE and polyurethane were well carbonized by the stabiliza-

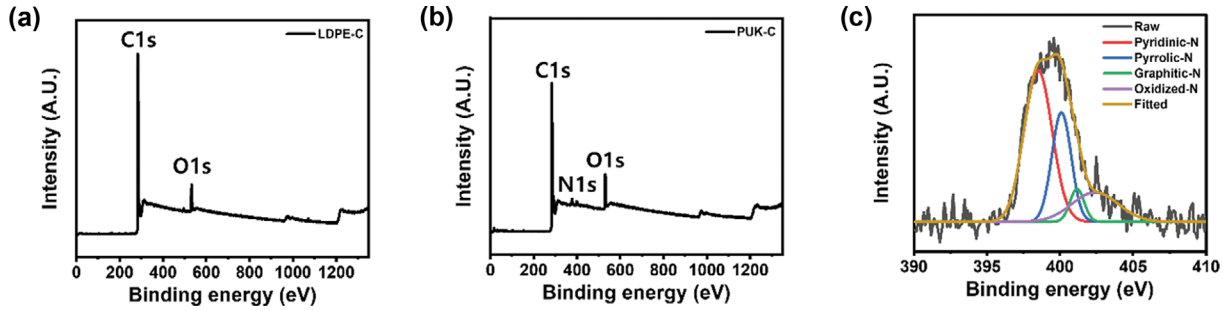

Fig. 3. XPS full range survey graphs of (a) LDPE-C and (b) PUK-C samples. (c) N1s XPS spectra of PUK-C sample.

Table 1. XPS analysis data of LDPE-C and PUK-C samples

	C (atomic %)	O (atomic %)	N (atomic %)
LDPE-C sample	92.89	7.11	0
PUK-C sample	88.39	9.8	1.8

tion and carbonization processes, and their properties measured after the processes, such as surface area, were considerably enhanced. In terms of nitrogen functional groups that promote the reactivity for redox reactions of vanadium ions, PUK-C sample contained them on its surface. The next crucial step is to evaluate whether these LDPE-C and PUK-C can act as electrochemical carbon catalysts to enhance the reactivity for redox reactions of vanadium ions, followed by the performance of VRFBs.

3. Electrochemical Analysis and Performance Evaluations of VRFBs

To investigate whether LDPE-C and PUK-C can act as electrochemical carbon catalysts, electrochemical analysis is conducted. Here, these carbon samples were doped onto GF electrodes to act as catalysts. The doping process was conducted by dispersing 20 mg of each carbon catalyst sample into 1 mL isopropyl alcohol (IPA) through sonification. The resulting solution was then uniformly doped onto the surface of GF electrode. To recognize whether the doping of carbon catalyst is well done, SEM analysis is performed (Fig. 4). Figs. 4(a) and 4(c) demonstrated that LDPE-C and PUK-C samples were effectively doped onto the surface of GF electrode. Furthermore, as depicted in Figs. 4(b) and 4(d), there were no noticeable structural differences between them. These observations confirmed that the targeted samples (LDPE-C and PUK-C) were successfully incorporated onto the surface of GF electrode.

To investigate the effects of catalysts doped GF electrodes on the reactivity for redox reactions of vanadium ions, electrochemical evaluations are conducted. According to Figs. 5(a) and 5(b), in CV curve measurements performed with vanadium electrolyte containing 0.015 M $VOSO_4$ dissolved in 3 M sulfuric acid, the reactivity for redox reaction of vanadium electrolyte was enhanced when both LDPE-C and PUK-C samples were employed as catalysts.

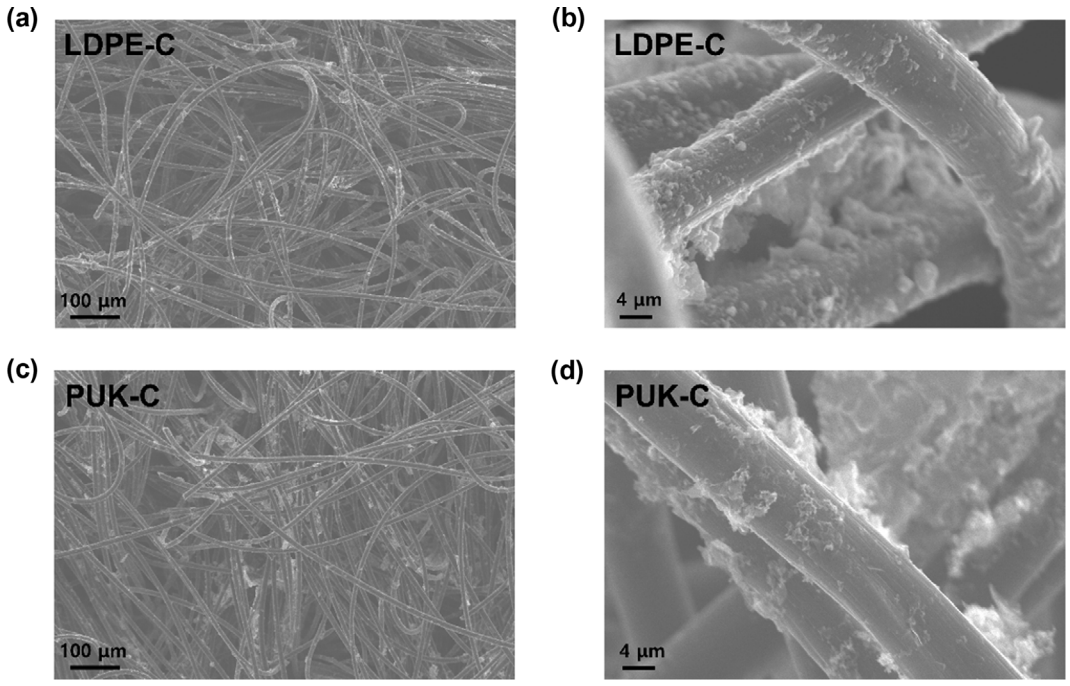

Fig. 4. SEM images of (a), (b) LDPE-C doped GF and (c), (d) PUK-C doped GF.

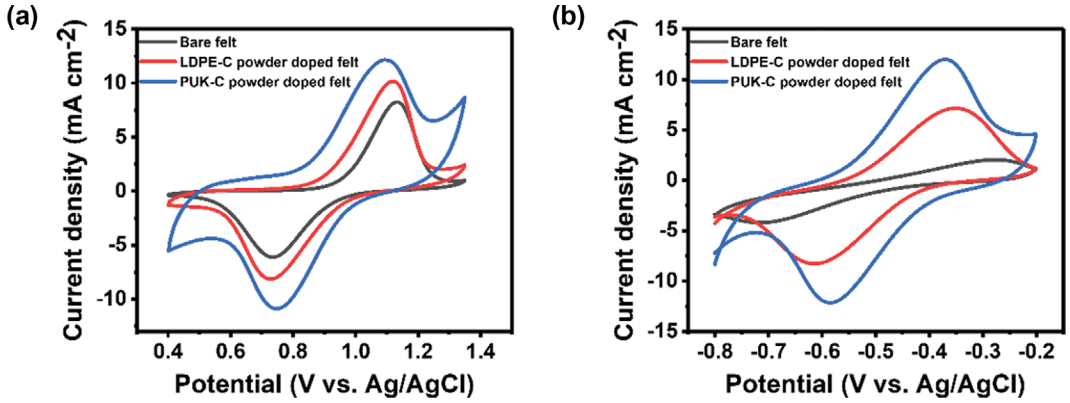

Fig. 5. CV curves of bare GF and catalysts doped GFs measured in (a) catholyte and (b) anolyte.

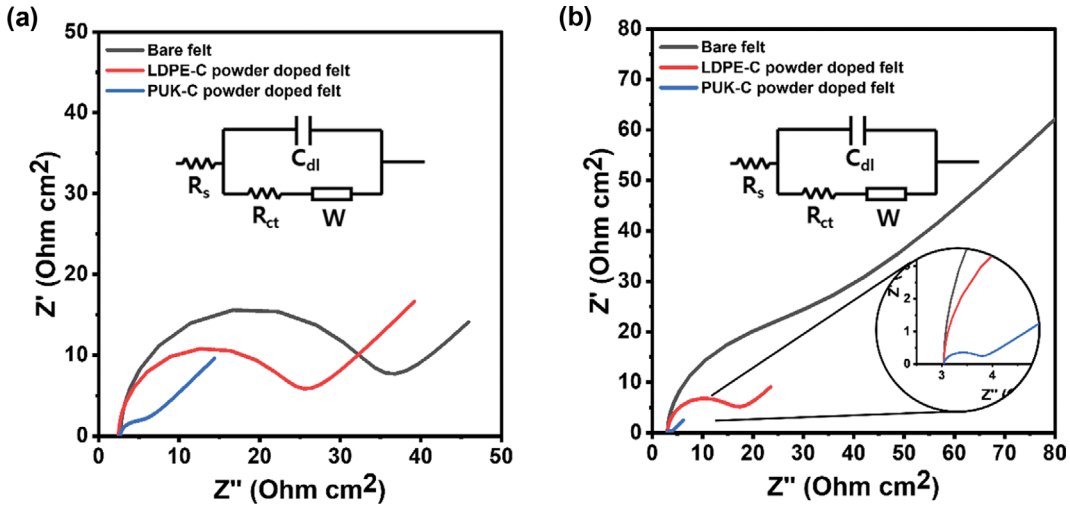

Fig. 6. Nyquist plots of bare GF and catalysts doped GFs measured in (a) catholyte and (b) anolyte.

Quantitatively, in catholyte, the peak current density and peak potential separation of LDPE-C doped GF electrode and PUK-C doped GF electrode increased by 23.4 and 47.6% (peak current density), and 2.5 and 12.5% (peak potential separation), when they were compared with those measured in bare GF electrode.

In anolyte, those of LDPE-C doped GF electrode and PUK-C doped GF electrode exhibited a significant increase of 250.5 and 487.3% (peak current density), and 40.9 and 50.0% (peak potential separation), when they were compared with those measured in bare GF electrode. These results indicated that the use of LDPE-C and PUK-C doped GF electrodes significantly improved the reactivity and overvoltage for redox reactions of vanadium electrolyte.

To further inspect the reactivity for redox reaction of vanadium ions, Nyquist plots are measured using EIS for each sample (Fig. 6(c) and 6(d)). In catholyte, charge transfer resistance (R_{ct}) occurring for the redox reaction for VO^{2+}/VO_2^+ of LDPE-C and PUK-C doped GF electrodes was reduced by 31.7 % (from 23.6 to 16.1 Ohm cm^2 (LDPE-C doped GF electrode)) and by 92.2% (from 23.6 to 1.85 Ohm cm^2 (PUK-C doped GF electrode)). In contrast, in anolyte, LDPE-C and PUK-C doped GF electrodes also exhibited a decrease in R_{ct} for the redox reaction of V^{2+}/V^{3+} by 51.2% (from 19.9 to 9.68 Ohm cm^2 (LDPE-C doped GF electrode)) and by 97.5% (from 19.9 to 0.49 Ohm cm^2 (PUK-C doped GF electrode)). These findings were evidence that the catalysts effectively enhanced the reactivity for redox reaction of vanadium ions. Notably, PUK-C was the most excellent catalyst among the tested samples.

The electrochemical evaluations corroborated that LDPE-C and PUK-C as catalysts were very effective to promote the redox reactions of vanadium ions. This improvement is probably attributed to the increased specific surface area, because this provides more effective active sites for the redox reactions of vanadium ions. As mentioned earlier, PUK-C sample exhibited a better reactivity than LDPE-C sample. This is due to its higher specific surface area and more proportion of nitrogen functional groups. This is evidence that the carbon catalysts derived from waste plastics are suitable for promoting the redox reactions of vanadium ions used for VRFBs.

To estimate the effects of catalysts doped GF electrodes on the performance of VRFBs, VRFB single cell tests were conducted using the catalysts doped GF electrodes. First of all, the step tests were conducted. For doing that, applied current density was changed from 80 to 250 mA cm^{-2}, and then, the current density was again returned to 80 mA cm^{-2} (Fig. 7). They showed that energy efficiency (EE) of VRFBs using LDPE-C and PUK-C doped GF electrodes was improved. At 20 mA cm^{-2}, EE of VRFB using bare felt electrode

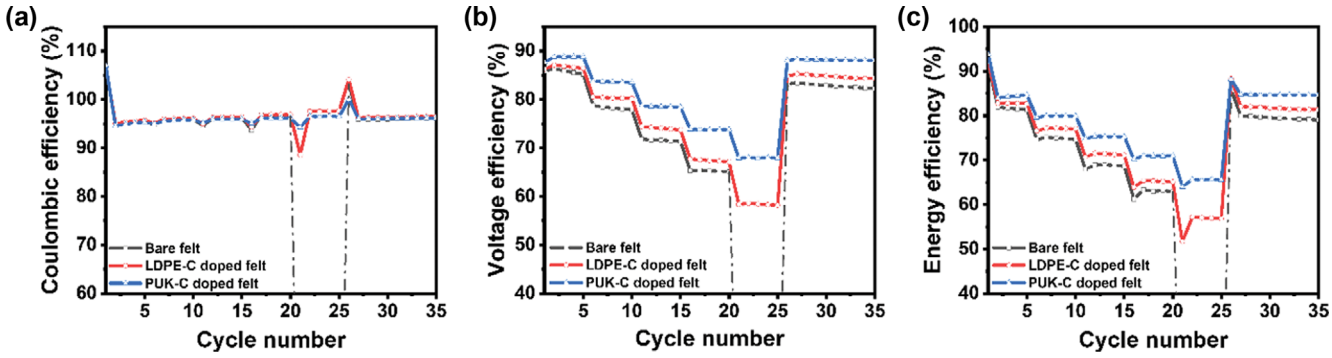

Fig. 7. (a) CE, (b) VE, and (c) EE graphs of VRFBs using bare GF and catalysts doped GFs measured at current densities of 80, 120, 160, 250 and 80 mA cm^{-2}.

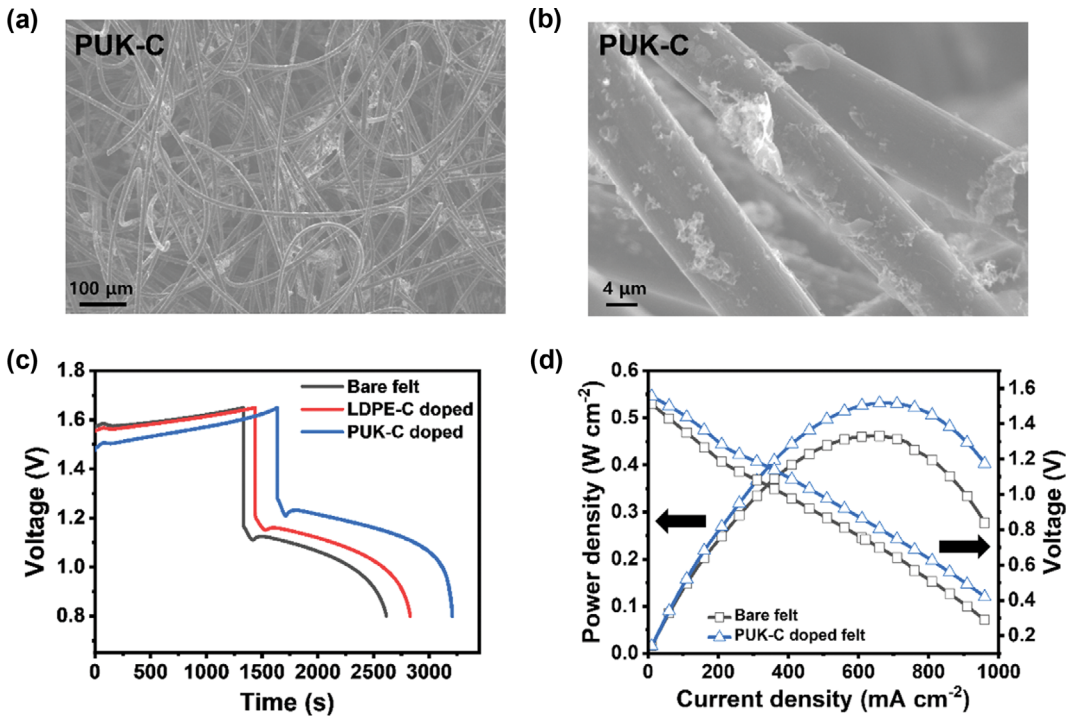

Fig. 8. SEM images (a), (b) PUK-C doped GF after RFB cycling test. (c) Charge and discharge curves and (d) polarization curves of VRFBs using care GF and catalysts doped GFs. The current density applied for measuring charge and discharge curves was 200 mA cm^{-2}.

was 62.7%, while that of VRFBs using LDPE-C and PUK-C doped GF electrodes was 65.0 and 70.8%, respectively. Specifically, even at 250 mA cm^{-2}, which corresponds to high and harsh current density condition, VRFB using bare felt did not work. However, EE of VRFBs using LDPE-C and PUK-C doped GF electrodes was 55.9 and 65.2%. Notably, this is another critical evidence that VRFB using PUK-C doped GF electrode exhibited the highest EE among the other tested options.

To ensure whether catalyst was stuck to electrode well even after step test, optimal inspection of PUK-C doped felt was conducted using SEM after step test. As demonstrated in Figs. 8(a) and 8(b), the catalyst attached to the felt surface remained unchanged even after step test. This indicates that this catalyst is well attached to the surface of electrode irrespective of the use of binder even after step test.

To further evaluate the effects of catalysts doped GF electrodes on the performance of VRFBs, the charge and discharge curves of VRFBs operated under high current density condition of 200 mA cm^{-2} are measured (Fig. 8(c)). As shown in Fig. 8(c), VRFB using bare felt electrode showed a higher overvoltage than VRFBs using other catalysts doped GF electrodes. This means that the former induces a shorter charging step than the latter. In contrast to this, the overvoltage of VRFB using PUK-C doped GF electrode was low, and this enabled a longer cycling of VRFB. In contrast to this, the cycle time of VRFB using LDPE-C doped GF electrode was placed between that of the other two VRFBs.

Regarding the discharging performance of VRFBs, MPD of all the tested VRFBs was measured to compare the performance of VRFBs using bare felt and PUK-C doped felt (Fig. 8(d)). According to Fig. 8(d), as current density increased, the power density of

VRFB using PUK-C doped felt also increased. More specifically, that of VRFB using bare felt was 0.46 W cm^{-2} at 640 mA cm^{-2}, while that of VRFB using PUK-C doped felt was 0.53 W cm^{-2} at 670 mA cm^{-2}. Conclusively, carbon materials prepared from plastics were suitable catalysts for increasing the performance of VRFBs using them. In particular, PUK-C catalyst was most effective one. This is because this PUK-C catalyst has a large portion of nitrogen functional groups and large surface area.

CONCLUSION

In this study, we successfully produced valuable carbon catalysts by recycling plastics and utilized them as catalysts for VRFBs. For preparing LDPE-C catalyst, LDPE was initially chemically treated as stabilization stage, and then, carbonized as the LDPE-C by heat treatment performed at 900 °C. Meanwhile, PUK-C catalyst was also produced by carbonizing polyurethanes at 800 °C with the addition of potassium carbonate. The structural properties of these final LDPE-C and PUK-C catalysts, were evaluated using BET and XPS analysis. The BET analysis revealed the specific surface areas of LDPE-C and PUK-C catalysts was 256.4 and 297.5 m^2 g^{-1}. Furthermore, by XPS analysis, some nitrogen functional groups were observed on the surface of PUK-C catalyst. As next, the electrochemical properties of these carbon catalysts were comprehensively assessed. When LDPE-C powder was doped onto GF electrode, the peak current density increased 23.4 and 250.5% at anode and cathode, while its peak potential separation was decreased by 2.5 and 40.9%. When PUK-C powder was doped onto GF electrode, even more remarkable improvements were observed with peak current density of 47.6 and 487.3% at anode and cathode, while its peak potential separation was decreased by 12.5 and 50.0%. Additionally, Nyquist plots were measured to calculate the R_{ct} occurring for the redox reactions of vanadium ions. According to the R_{ct} data, in catholyte, R_{ct} of LDPE-C and PUK-C doped GF electrodes was reduced for the redox reaction of VO^{2+}/VO_2^+ by 31.7 and 92.2%. In anolyte, LDPE-C and PUK-C doped GF electrodes also showed a decrease in R_{ct} for the redox reaction of V^{2+}/V^{3+} by 51.2 and 97.5%. Then, the performance of VRFBs using the catalysts was measured. According to the measurements, EE of VRFBs using LDPE-C and PUK-C doped GF electrodes was more enhanced than that of VRFBs measured without the catalyst by 2.3 and 8.1%, respectively. These results provide a strong evidence to support the conclusion that these plastic-based carbon catalysts are highly effective in enhancing the performance of VRFBs using them.

ACKNOWLEDGEMENTS

This study was supported by the Research Program funded by the SeoulTech (Seoul National University of Science and Technology).

REFERENCES

1. Z. Yang, J. Zhang, M. C. W. Kintner-Meyer, X. Lu, D. Choi, J. P. Lemmon and J. Liu, *Chem. Rev.*, **111**, 3577 (2011).
2. H. Chen, T. N. Cong, W. Yang, C. Tan, Y. Li and Y. Ding, *Prog. Nat. Sci.*, **19**, 291 (2009).
3. G. Park, S. Eun, W. Lee, D. Henkensmeier and Y. Kwon, *J. Power Sources*, **569**, 233015 (2023).
4. W. Lee, G. Park, D. Chang and Y. Kwon, *Korean J. Chem. Eng.*, **37**, 2326 (2020).
5. C. Chu, B. W. Kwon, W. Lee and Y. Kwon, *Korean J. Chem. Eng.*, **36**, 1732 (2019).
6. H. Lim, M. Shin, C. Noh, E. Koo, Y. Kwon and K. Y. Chung, *Korean J. Chem. Eng.*, **39**, 3146 (2022).
7. M. Chen, P. Liu, Y. Li, Y. Hu, Z. Hu and Q. Wang, *J. Therm. Anal. Calorim.*, **147**, 4131 (2022).
8. W. Lee, G. Park, D. Schröder and Y. Kwon, *Korean J. Chem. Eng.*, **38**, 1 (2022).
9. K. Hyun, M. Shin and Y. Kwon, *Korean J. Chem. Eng.*, **39**, 3315 (2022).
10. J. Ji, C. Noh, M. Shin, S. Oh, Y. Chung, Y. Kwon and D.-H. Kim, *Appl. Surf. Sci.*, **611**, 155665 (2023).
11. H. An, C. Noh, S. Jeon, Y. Kwon and Y. Chung, *J. Energy Storage*, **68**, 107796 (2023).
12. S. Jeon, H. An, C. Noh, Y. Kwon and Y. Chung, *Appl. Surf. Sci.*, **613**, 155962 (2023).
13. W. Lee, C. Jo, S. Youk, H. Y. Shin, J. Lee, Y. Chung and Y. Kwon, *Appl. Surf. Sci.*, **429**, 187 (2018).
14. C. Noh, B. W. Kwon, Y. Chung and Y. Kwon, *J. Power Sources*, **406**, 26 (2018).
15. C. Noh, C. S. Lee, W. S. Chi, Y. Chung, J. H. Kim and Y. Kwon, *J. Electrochem. Soc.*, **165**, A1388 (2018).
16. H. An, C. Noh, S. Jeon, M. Shin, Y. Kwon and Y. J. Chung, *Int. J. Energy Res.*, **46**, 11802 (2022).
17. Y. Chung, C. Noh and Y. Kwon, *J. Power Sources*, **438**, 227063 (2019).
18. S. Oh, C. Noh, M. Shin and Y. Kwon, *Int. J. Energy Res.*, **46**, 8803 (2022).
19. Y.-R. Dong, Y. Kawagoe, K. Itou, H. Kaku, K. Hanafusa, K. Moriuchi and T. Shigematsu, *ECS Trans.*, **75**, 27 (2017).
20. P. K. Leung, C. Ponce-De-León, C. T. J. Low, A. A. Shah and F. C. Walsh, *J. Power Sources*, **196**, 5174 (2011).
21. Q. Li, A. Bai, T. Zhang, S. Li and H. Sun, *R. Soc. Open Sci.*, **7**, 200402 (2020).
22. V. Mahanta, M. Raja and R. Kothandaraman, *Mater. Lett.*, **247**, 63 (2019).
23. G. J. W. Radford, J. Cox, R. G. A. Wills and F. C. Walsh, *J. Power Sources*, **185**, 1499 (2008).
24. H. M. Lee, K. H. An and B. J. Kim, *Carbon Lett.*, **15**, 146 (2014).
25. M. Ulaganathan, A. Jain, V. Aravindan, S. Jayaraman, W. C. Ling, T. M. Lim, M. P. Srinivasan, Q. Yan and S. Madhavi, *J. Power Sources*, **274**, 846 (2015).
26. Y. Lian, M. Ni, Z. Huang, R. Chen, L. Zhou, W. Utetiwabo and W. Yang, *Chem. Eng. J.*, **366**, 313 (2019).
27. H. Lim, M. Shin, C.-G. Phae and Y. Kwon, *Chem. - An Asian J.*, **17**, e202200754 (2022).
28. D. Choi, D. Jang, H. I. Joh, E. Reichmanis and S. Lee, *Chem. Mater.*, **29**, 9518 (2017).
29. X. Zhang, Z. Lin, C. Qin, X. Guo, Y. Ma and X. Jiang, *J. Mater. Sci. Mater. Electron.*, **31**, 715 (2020).
30. R. Wang, Z. Tan, W. Zhong, K. Liu, M. Li, Y. Chen, W. Wang and D. Wang, *Compos. Commun.*, **22**, 100426 (2020).

31. S. Xiao, S. Liu, J. Zhang and Y. Wang, *J. Power Sources*, **293**, 119 (2015).
32. W. Li, K. Wang, Z. Li, C. Sun, S. Zhao, D. Zhang, K. Chen and A. Guo, *New J. Chem.*, **46**, 23328 (2022).
33. G. Nam, S. Choi, H. Byun, Y.-M. Rhym and S. E. Shim, *Macromol. Res.*, **21**, 958 (2013).
34. W. Chen, G. Zhang, D. Li, S. Ma, B. Wang and X. Jiang, *Ind. Eng. Chem. Res.*, **59**, 7447 (2020).
35. L. Shi, S. Liu, Z. He and J. Shen, *Electrochim. Acta*, **138**, 93 (2014).
36. M. E. Lee, H.-J. Jin and Y. S. Yun, *RSC Adv.*, **7**, 43227 (2017).
37. J. Jin, X. Fu, Q. Liu, Y. Liu, Z. Wei, K. Niu and J. Zhang, *ACS Nano*, **7**, 4764 (2013).
38. M. Chen, P. Liu, Y. Li, Y. Hu, Z. Hu and Q. Wang, *J. Therm. Anal. Calorim.*, **147**, 4131 (2022).
39. L. Wang, F. Sun, F. Hao, Z. Qu, J. Gao, M. Liu, K. Wang, G. Zhao and Y. Qin, *Chem. Eng. J.*, **383**, 123205 (2020).
40. J. Hayashi, T. Horikawa, K. Muroyama and V. G. Gomes, *Micropor. Mesopor. Mater.*, **55**, 63 (2002).
41. M. Galhetas, A. S. Mestre, M. L. Pinto, I. Gulyurtlu, H. Lopes and A. P. Carvalho, *J. Colloid Interface Sci.*, **433**, 94 (2014).
42. I. I. Gurten, M. Ozmak, E. Yagmur and Z. Aktas, *Biomass Bioenergy*, **37**, 73 (2012).
43. D. Adinata, W. M. A. Wan Daud and M. K. Aroua, *Bioresour. Technol.*, **98**, 145 (2007).
44. Y. Shao, X. Wang, M. Engelhard, C. Wang, S. Dai, J. Liu, Z. Yang and Y. Lin, *J. Power Sources*, **195**, 4375 (2010).
45. X. Yan, T. Xu, G. Chen, S. Yang, H. Liu and Q. Xue, *J. Phys. D Appl. Phys.*, **37**, 1 (2004).
46. X. Zhang, Q. Fan, N. Qu, H. Yang, M. Wang, A. Liu and J. Yang, *Nanoscale*, **11**, 8588 (2019).
47. M. Shin, C. Noh, Y. Chung, D. H. Kim and Y. Kwon, *Appl. Surf. Sci.*, **550**, 148977 (2021).